0031-3998/95/3804-0485$03.00/0
PEDIATRIC RESEARCH

Vol. 38, No. 4, 1995
Printed in U.S.A.

Int-2 Influences the Development of the Nodose Ganglion

FENG QIN AND MARGARET L. KIRBY

Department of Cellular Biology and Anatomy, Heart Development Group, Medical College of Georgia, Augusta, Georgia 30912-20000

ABSTRACT

The *int-2* gene was first described as a common proviral integration site in tumors induced by mouse mammary tumor virus (MMTV). During embryonic development *int-2* is produced and released by cells in the rhombencephalon and diffuses to the ectoderm to induce formation of the otocyst from the otic placode. *Int-2* also influences the development of the vestibulocochlear ganglion that is derived from the otic placode. During embryogenesis the otic and nodose placodes, primordia of the inner ear and the nodose ganglia, respectively, are located adjacent to each other in the embryonic ectoderm. The nodose ganglia provide sensory innervation to all of the viscera. Using Northern analysis we determined that a high level of *int-2* is transcribed in stage 14 chick embryos. This is the time when cells begin to migrate from the nodose placodes to form the nodose ganglia. Using human and mouse sequences to design primers around the translation start site of the transcript, a partial clone containing the translation start site of chick *int-2* was obtained by polymerase chain reaction amplification from chick genomic DNA and cloned. An antisense oligodeoxynucleotide was designed to the region of the translation start site, and *in vitro* and *in vivo* techniques were used to demonstrate that inhibition of *int-2* translation using this antisense oligonucleotide causes delayed and abnormal development of the nodose placodes. For *in vitro* studies, explants of stage 12 chick embryos containing neural tube, adjacent surface ectoderm, and pharyngeal endoderm were cultured with *int-2* antisense oligonucleotide. For the *in vivo* studies, pieces of resin impregnated with *int-2* antisense oligonucleotide were implanted into the neural tube of stage 12 chick embryos at the level of the otic and nodose placodes. We found that the development of the nodose placodes exposed to *int-2* antisense oligodeoxynucleotide was delayed and abnormal. These differences were not seen in embryos or explants treated with similar concentrations of sense or nonspecific oligomers. Western analysis and immunohistochemistry showed that an *int-2*-immunoreactive protein was reduced in the pharyngeal region and nodose ganglia of the embryos exposed to *int-2* antisense oligodeoxynucleotide, whereas it was not affected in embryos treated with sense oligomer. We conclude that *int-2* may be necessary for normal development of the nodose ganglia. (***Pediatr Res* 38: 485–492, 1995**)

Abbreviations

FGF, fibroblast growth factor
PCR, polymerase chain reaction
TST, Tris-saline-Triton

The *int-2* gene was originally discovered through its transcriptional activation by mouse mammary tumor virus and is classified as a proto-oncogene (1, 2). Sequence analysis showed *int-2* to be a member of the FGF family (3). The FGF family currently has seven members that share 30–60% amino acid sequence similarity over a 120-amino acid central core region (4). Many members of this family are important in development. *Int-2* is rarely expressed in adult tissues but displays complex expression patterns during embryogenesis (2, 5). In mouse embryos, *int-2* transcripts have been detected in the rhombencephalon. *Int-2* is also expressed in parietal endoderm, early migrating mesoderm, a portion of the pharyngeal pouches, and neuroepithelium of the hindbrain during gastrulation and neurulation (6, 7). It is thought that *int-2* may influence cell transformation from ectoderm to mesoderm (8). In the chick embryo, *int-2* is localized in the rhombencephalon at stage 14 and later disappears from the rhombencephalon and is expressed in the otocyst. Using human *int-2* antibody and antisense oligodeoxynucleotide, Represa *et al.* (9) inhibited formation of the otic vesicle which is the primordium of the inner ear. These studies were carried out *in vitro*. Part of the effect of *int-2* protein suppression was due to a decrease in the cell proliferation rate of the otic placode during the formation of the otocyst (9).

During the early development of vertebrates, a series of ectodermal thickenings cover the head and pharyngeal region (10, 11). They are called epipharyngeal placodes. Along with the neural crest, they will give rise to peripheral sensory ganglia. It has been speculated that *int-2* expression is necessary for the development of most of the epipharyngeal pla-

Received September 21, 1994; accepted June 6, 1995.
Correspondence and reprint requests to: Dr. Margaret L. Kirby, Department of Cellular Biology and Anatomy, Medical College of Georgia, Augusta, GA 30912-2000.
Supported by a grant from the Georgia Affiliate of the America Heart Association.

codes. A mutant mouse with *int-2* knockout has been reported in which homozygotes had defective development of the inner ear and facioacoustic ganglia, both of which are derived from the otic placode (12). Mice lacking *int-2* die suddenly soon after birth of an unknown cause. Nodose ganglia, which provide sensory innervation to the heart, are derived from the nodose placodes, the ectodermal placodes located just caudal to the otic placodes during embryogenesis. Cell migration from the nodose placodes to form the nodose ganglia occurs around stage 14 in the chick embryo (13). The formation of the otocyst and migration of precursors of the nodose ganglia occur within a period of a few hours.

We have been interested in factors common to the development of the otic and nodose placodes and their derivatives because of a surgical model of long QT with deafness created in this laboratory by ablation of the otic and nodose placodes (14, 15). The long QT with deafness syndrome was first clinically described by Jervell and Lange-Nielsen (15, 16). It has been estimated that 1% of deaf people have a form of long QT. Other patients have been identified with inherited prolonged QT interval in the ECG without the associated congenital deafness (17). Long QT can be associated with syncope that can cause loss of consciousness and death. The embryologic association of the otic and nodose placodes provides one potential mechanism for the pathogenesis of long QT interval on the ECG in conjunction with congenital deafness.

To determine whether *int-2* affects the development of the nodose ganglia, we used *int-2* antisense oligodeoxynucleotide *in vitro* and *in vivo* to block the translation of *int-2* protein. Since neither the avian DNA sequence nor protein or antibody is currently available, we cloned a portion of the chick *int-2* gene. Cloning of a PCR fragment containing the translation start site of *int-2* message confirmed that this region is very similar in mouse and chick. We determined that a decrease in expression of *int-2*-like protein is associated with abnormal development of the nodose ganglia. This finding is significant in that it provides a common molecular basis for abnormal development of the ear and innervation of the heart, and could provide an etiology for long QT with congenital deafness syndrome.

METHODS

Animals. Fertilized Arbor Acre chicken eggs (Seaboard Farms, Athens, GA) were obtained fresh and stored at 18–20°C until incubation. Eggs were incubated in forced-draft incubators maintained at 70% humidity and 37°C, and were opened on a horizontal disk sander after 42–45 h incubation. The embryos were stained with neutral red-impregnated agar and staged according to the Hamburger-Hamilton staging procedure.

Northern analysis. Whole embryos were collected at different stages of development and frozen in guanidium hydrochloride. Total RNA was extracted by homogenization in RNAzol. The polyadenylated RNA was purified by oligo(dT) chromatography. The mRNA (2.5 μg) was then separated on a formaldehyde-agarose denaturing gel and transferred to Hybond-N. Fixation of RNA was accomplished by exposure to UV light for 2–3 min. Mouse *int-2* DNA oligolabeled with P^{32} was used as a probe (gift of Dr. Mansour). The filter was hybridized in 20% formamide at 52°C and washed to a final stringency of 1 × SSC at 55°C. The filter was exposed to Kodak Omat-AR x-ray film at 70°C for 24 h. An 18S riboprobe (Ambion) was used as an internal standard to establish the amount of RNA in each sample. The hybridized bands were quantified by densitometry of the autoradiogram.

Cloning of a PCR fragment of chick int-2. The 5′ region of the *int-2* chicken gene containing the translation start site was amplified using PCR technique. The site to be amplified was chosen using a conserved region of human and mouse *int-2* sequences that is located in the first exon. The forward primer is located upstream of AUG translation start codon. The reverse primer is located at 3′ end of the first exon (see Fig. 3).

The primers were:

Forward: 5′ ATGCCGGGATGGGCCTGATC 3′

Reverse: 5′ AGGCGCTGTTCTCAAGGCTG 3′

Chick genomic DNA was used as a template. The PCR was performed as follows: initial denaturation at 95°C for 5 min, followed by 35 cycles of 94°C for 1 min, 58°C for 1 min, and 72°C for 45 s. A 220-bp PCR product that hybridized positively with the mouse *int-2* probe was subcloned into pBluescript SK (Promega, Madison, WS), by blunt-end ligation. The sequence of the clone was determined using the Sequenase sequencing kit, and the reaction products were separated on an IBI Sequencing Gel Apparatus. The sequence was read manually and entered into PC/Gene software for sequence comparisons.

Oligonucleotides. The *int-2* antisense oligodeoxynucleotide was designed to complement the 15 nucleotides beginning at the AUG translation start site of the chick int-2 message. A corresponding chick *int-2* sense oligodeoxynucleotide was used as one control, and a second control consisted of the nucleotides in the antisense oligo rearranged in random order:

Int-2as (antisense): 5′-CCAGATTAGGCCCAT-3′

Int-2s (sense): 5′-ATGGGCCTAATCTGG-3′

Int-2r (random): 5′-CACTGCCATTCGAAG-3′

The oligodeoxynucleotides were synthesized by the Molecular Biology Core Facility at the University of Georgia (Athens, GA), and were phosphorothioate-modified to enhance their half-life. GenBank™ was searched with each oligodeoxynucleotide to determine the probability that the oligodeoxynucleotide would cross-hybridize with messages other than the one targeted. No other potential messages were identified.

Culture of Explanted Tissue. Explants were prepared from stage 12 chick embryos that were microdissected in sterile conditions using incisions through the planes indicated in Figure 1. The explants were incubated in culture medium M-199 with added *int-2* antisense oligodeoxynucleotide (20 mM) for 120 min. Each explant was then transferred to an agar gel-coated surface (0.2% in M-199) in the bottom of a 16-mm well and incubated in M-199 with Earle's salts at 37°C in 5% CO_2, for 18–20 h. Ten percent FCS was added to the medium and the pH was maintained at 7.2.

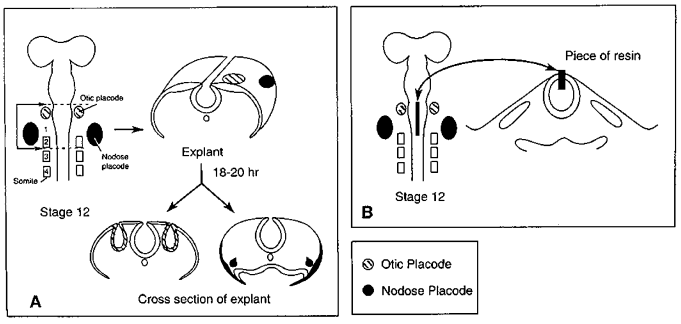

Figure 1. Experimental design *in vitro* (*A*) and *in vivo* (*B*). *A*, Explants were prepared from stage 12 chick embryos by cutting across the embryo at the sites indicated by the dashed line, submerged in 0.2% agar and incubated in M-199 with Earle's salts at 37°C in 5% CO_2 for 18–20 h. During the time in culture, the otic placodes invaginate to form the otocyst, and cell migration from the nodose placodes forms the nodose ganglia. *B*, Rectangular pieces of AG-501 X8 Resins impregnated with oligonucleotide were implanted into the rhombencephalon at the level of the otic and nodose placodes of stage 12 chick embryos.

Treatment of embryos in vivo. Resin beads (AG-501 X8, Bio-Rad, Richmond, CA) were cut into rectangular pieces (20–50-μm width, 20–50-μm depth, 600-μm length). These pieces were incubated in *int-2* antisense oligodeoxynucleotide (80 mM) at 4°C overnight, and were then implanted into the rhombencephalon of stage 12 chick embryos at the level of the otic and nodose placodes (Fig. 1). The embryos were harvested one, two and three days after implantation of the impregnated resin.

Histologic analysis. The explants and embryos were fixed in Carnoy's fixative, dehydrated in a series of alcohols and embedded in paraffin. Sections were cut at 8 μm and stained with thionin. The sections were evaluated for the degree of development of the nodose ganglia and otocysts. The volume of each nodose ganglion was determined as follows: the area of the ganglion in each section was measured using Jandel Scientific (San Rafael, CA) Sigma scan software; each area was multiplied by the section thickness (8 μm); and the volumes of the ganglion for all the sections were totaled. Statistical analysis of the total volumes was done by one-way analysis of variance using GraphPAD InStat Software (version 1.12a). *Post hoc* tests were done by the Bonferroni method using the same software. A difference was considered significant if the p value was less than 0.05.

Western analysis. Lysates were prepared by homogenizing the pharyngeal region of embryos in homogenizing buffer that consisted of 0.5 M NaCl, 20 mM Tris, 3 mM EDTA, and 0.1 mM phenylmethylsulfonyl fluoride. The samples were centrifuged (18,000 rpm) for 2 h at 4°C. Total protein in the lysate was quantified using the BCA protein assay (Pierce, Rockford, IL) with BSA as a standard. For each sample, 75 μg of protein were resolved on a 12% polyacrylamide gel. The proteins were transferred to a BA-S nitrocellulose membrane. Human *int-2* antibody (diluted 1:1000, Cambridge Research Biochemicals, UK) was used as the primary antibody. peroxidase-conjugated rabbit IgG (diluted 1:1000; Organon Teknika Co., West Orange, NJ) was used as the secondary antibody. Visualization was accomplished by reaction of Tris-buffered saline/4-chloronaphthol/H_2O_2. Molecular weights were calculated by direct comparison with prestained broad molecular weight markers (Bio-Rad).

Immunostaining. For whole-mount immunostaining, the embryos were fixed in 4% paraformaldehyde overnight at 4°C, followed by immersion in methanol for 2 days at −20°C and then in 50% methanol/50% DMSO for 4 min on ice. The embryos were treated with 1% periodic acid/distilled water for 30 min to inhibit endogenous peroxidase. After washing in TST, they were incubated with primary antibody (mouse 68-kD neurofilament MAb; Sigma) in TST containing 5% milk for 2 days at 4°C. The embryos were then incubated in secondary antibody (horseradish peroxidase-conjugated rabbit anti-mouse IgG) for 2 days after washing 3 h in TST. Visualization was accomplished by DAB reaction for horseradish peroxidase.

For immunohistochemistry, embryos were fixed in 4% paraformaldehyde overnight, dehydrated in a series of alcohols, and embedded in paraffin. Sections were cut at 12 μm and mounted on serine-coated slides. The sections were deparaffinized in xylene and hydrated in a graded alcohol series. Human *int-2* antibody was used as the primary antibody and peroxidase-conjugated rabbit IgG was used as secondary antibody. Both antibodies were diluted 1:1000. Fetal bovine serum was used to block nonspecific binding. The sections were reacted with a DAB/imidazole/H_2O_2 solution and counterstained in hematoxylin.

RESULTS

Northern blot analysis was carried out using different stages of chick embryos to determine when the highest levels of *int-2* message were present. We used cross-species hybridization with mouse *int-2* cDNA as the probe, under moderately stringent hybridization conditions (20% formamide, 52°C with washes to a final stringency of 1 × SSC at 52°C). Two predominant species of *int-2* RNA were observed with estimated sizes of 3.0 and 1.9 kb which correspond to the message sizes described for mouse and *Xenopus*. The expression of *int-2* varied from stage 10 to stage 36. The ratio of densities of *int-2*/18S showed an increasing level of the *int-2* message from stage 10 to stage 14. The highest level of expression was at stage 14 (Fig. 2). This stage corresponds to the time of otocyst closure and migration of cells from the nodose placodes to form the nodose ganglia (12). After stage 14 the level of expression decreased. Thus the temporal pattern of *int-2* expression is such that it is at a high level preceding and during the events to be examined in this study.

To design an antisense oligonucleotide that would bind with an appropriate region of the *int-2* message for inactivation, the 5′ region of the chick message was cloned using PCR. The primers were designed to identify a region with a high degree of conservation between the human and mouse *int-2* sequences which is located in the first exon region. Using chick genomic DNA as a template, a PCR fragment of expected size (Fig. 3; 220 bp) was amplified. The same size band was also amplified when using chick stage 14 cDNA as a template. A Southern blot using mouse *int-2* cDNA as probe showed the fragment hybridized strongly with *int-2* DNA. This fragment was sub-

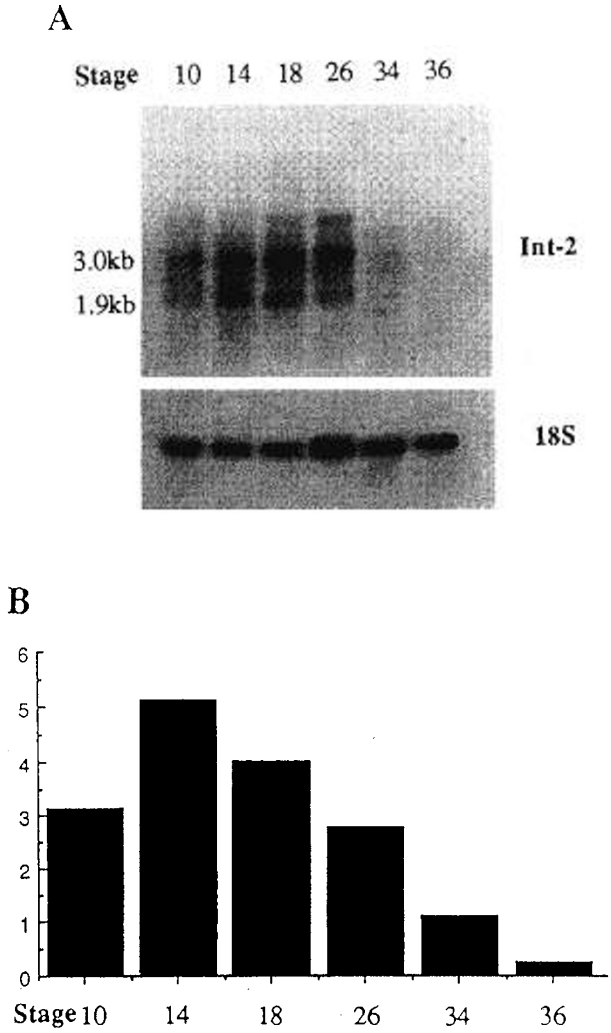

Figure 2. Northern blot analysis of *int-2* expression at different stages of chick embryo development. *A*, Mouse *int-2* DNA (open reading frame) as a probe identified two transcripts of 3.0- and 1.9-kb estimated size. An 18S RNA was used as an internal control. *B*, Ratio of densities of *int-2*/18S as measured by densitometer is indicated on the *y* axis. The result shows that *int-2* expression is highest in stage 14 chick embryos.

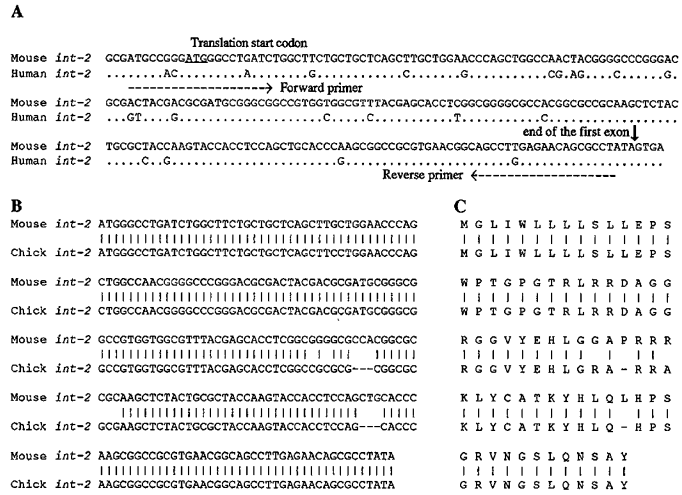

Figure 3. Cloning of a PCR fragment of chick *int-2*. *A*, Two PCR primers were designed using the first exon of mouse *int-2* which has high percentage similarity to human *int-2* in this region. *B*, Alignment of the nucleotide sequences of the PCR fragment of chick *int-2* with the corresponding region of mouse *int-2*. *C*, Alignment of the deduced amino acid sequences of chick and mouse *int-2*.

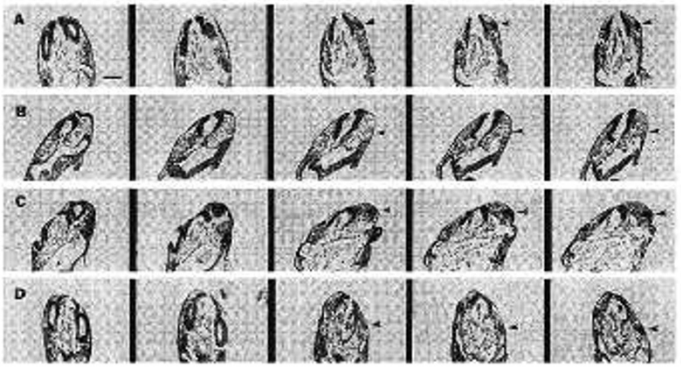

Figure 4. Development of the nodose placodes in explants. *A*, *B*, *C*, and *D* represent four groups of explants. Five sections in each type of explant from left to right represent section at otocyst to section at nodose ganglion. Cells migrated from the nodose placodes to form the nodose ganglia in normal explants after 18–20 h of culture (*A*). Cell migration was delayed and not obvious in the explants exposed to *int-2* antisense oligonucleotide (*B*). Explants exposed to *int-2* sense and random oligonucleotides (*C* and *D*) were used as controls. Cells migrated from nodose placodes to form nodose ganglia in these explants. The nodose placodes are indicated by the *arrowhead*. Bar = 250 μm.

cloned into pBluescript. Sequencing of the fragment showed it was 95% similar to mouse *int-2*. The *int-2* antisense oligonucleotide used in these experiments was a 15-mer complementary to the region of AUG translation start site (Fig. 3).

Explants were made using similar conditions to those reported by Represa *et al.* (9). The explants were incubated before plating in 20 mM phosphothioate-protected oligomers. In these explants, incubated without any oligomers or with the control oligomers, the nodose placodes became thickened and the cells delaminated from the surface ectoderm and migrated to form the nodose ganglia (Fig 4*A*). In 5 of 6 explants, cell migration from the nodose placodes did not occur after exposure to *int-2* antisense (Fig. 4*B*, Table 1). In 6 of 7 explants exposed to *int-2* sense oligonucleotides, cell migration from the nodose placodes occurred (Fig. 4*C*, Table 1). Treatment of 5 explants with random-ordered oligonucleotide resulted in normal formation of the nodose ganglia (Fig. 4*D*, Table 1).

Since the temporal and spatial windows of observation of effects of *int-2* antisense exposure are quite limited in explants,

Table 1. *Number of embryos with nodose defects*

	Nodose defects/number of embryos analyzed		
	Antisense	Sense	Random
In vitro	5/6	2/7	0/5
In vivo	14/20	0/18	0/13

the effect of *int-2* antisense on the formation of the nodose ganglion was also determined *in vivo*. A slice of resin bead impregnated with *int-2* antisense, sense or random-ordered oligodeoxynucleotide was implanted into the rhombencephalon at the level of the nodose placode in stage 12 embryos. The embryos were harvested one, 2 or 3 days after implantation of the bead. In the control groups, the formation of the nodose

ganglia was normal. The development of the nodose ganglion was delayed in 14 of the 20 embryos exposed to *int-2* antisense. In the embryos one day after implantation of the resin bead soaked in antisense oligodeoxynucleotide, cell migration from the nodose placodes was not obvious. In embryos two days after exposure to the antisense, some cells had migrated to form the ganglia. These ganglia were only 70% of the size of ganglia in the two control groups (Table 2A). At 3 days after exposure to the antisense the ganglia were still only 82% of the size of the ganglia in the control groups (Table 2B). Most notable though was the complete absence of any nerve trunks connecting the ganglia to the neural tube. By contrast the ganglia in both control groups had substantial vagus nerves connecting them to the neural tube (compare Fig. 5*a*, *b*, *c*, with *d*, *e*, *f*). To eliminate the possibility of defasciculation of the central process of the vagus nerve, whole-mount immunostaining of neurofilament was done. The nodose ganglia were not connected to the neural tube in embryos exposed to *int-2* antisense oligonucleotide (color plate, Fig. 6). A communication could be seen between the petrosal ganglion (glossopharyngeal distal ganglion) and the nodose ganglion. The glossopharyngeal ganglion also lacked a central process.

Given the phenotypic consequences of *int-2* antisense-treatment, it was important to determine the level of expression of *int-2* protein. Since a chick antibody for *int-2* is currently not available, we used the antibody for human *int-2*. Western blot analysis of stage 18 chick embryos showed a 27.5-kD band. This is the same molecular mass as reported for the *int-2* protein in mammals. The protein recognized by this antibody was dramatically reduced in embryos exposed to *int-2* antisense compared with embryos exposed to *int-2* sense oligodeoxynucleotide, with the same amount of total protein (Fig. 7).

Since the human *int-2* antibody appeared to identify *int-2* protein on Western analysis, we attempted peroxidase/antiperoxidase immnunohistochemistry using human *int-2* antibody on sections of stage 14 and18 embryos. At stage 12, faint *int-2* immunoreactivity could be seen in the caudal rhombencephalon and otic placode, as reported previously by Wilkinson *et al.* (8). At this stage no reactivity could be detected in the nodose placode (data not shown). At stage 18, the *int-2* immunoreactivity could be seen in the pharyngeal endoderm, pharyngeal ectoderm, dorsal neural tube and nodose ganglia. It was no longer visible in the hindbrain. Stage 18 embryos exposed to *int-2* antisense at stage 12, had decreased amounts of the reaction product in the pharyngeal endoderm and ectoderm as well as the nodose ganglia, compared with normal embryos and embryos exposed to *int-2* sense oligodeoxynucleotide (color plate, Fig. 8).

Table 2. *Nodose ganglion size with treatment*

	Int-2 antisense	*Int-2* sense	*Int-2* random
A. Size 48 h after treatment (mm × 10^{-4})			
Mean	7.17*	10.19	10.72
SD	1.13	1.21	1.17
SEM	0.43	0.46	0.44
B. Size 72 h after treatment (mm × 10^{-3})			
Mean	1.65*	2.01	2.03
SD	0.14	0.15	0.14
SEM	0.05	0.06	0.05

* $p < 0.01$ *versus int-2* sense group and $p < 0.001$ *versus int-2* random group.

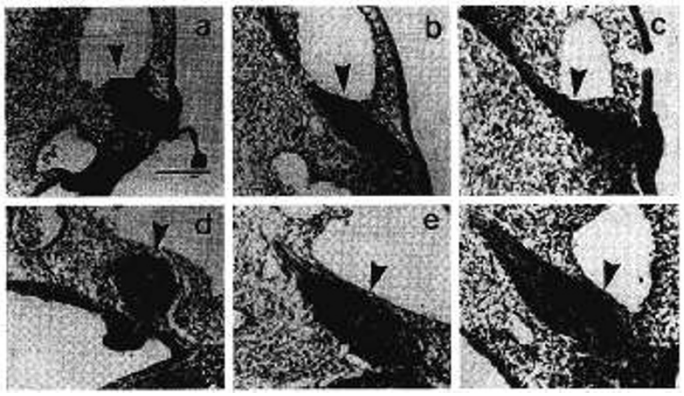

Figure 5. Development of the nodose ganglia in embryos exposed to *int-2* antisense oligonucleotide *in vivo*. The formation of the nodose ganglia was delayed and the ganglia failed to connect with the neural tube by a nerve trunks (vagus nerve) in embryos exposed to *int-2* antisense oligonucleotide (*a* and *d*). The development of the nodose ganglia was normal in embryos exposed to *int-2* sense (*b* and *e*) and random oligonucleotides (*c* and *f*). *a*, *b*, and *c* are embryos two days after surgery. *d*, *e*, and *f* are embryos 3 days after surgery. The nodose ganglia are indicated by the *arrowhead*. Bar = 80 μm.

DISCUSSION

Represa *et al.* (9) suggested that all of the postotic placodes might require *int-2* for normal development. Mansour *et al.* (12) supported and extended this hypothesis by showing that development of the inner ear and facioacoustic ganglia in the *int-2* mutant mouse is abnormal. Our results indicate a potential role for *int-2* in development of the nodose ganglion which is derived from the epipharyngeal placode immediately caudal to the otic placode. The major period of neuron generation of the nodose ganglia occurs before d 5 of incubation, and loss of approximately half of the neurons in the ganglion occurs between d 5 and 12 (18). We observed the morphologic characteristics of the nodose ganglia on incubation d 3, 4, and 5 after the embryos were exposed to *int-2* antisense oligodeoxynucleotide on d 2 of incubation. In this period, the nodose ganglia should undergo their major increase in size and cell number; however, we found that in embryos exposed at a single point in early development to *int-2* antisense oligonucleotide, the nodose ganglia formed later and were significantly smaller than those in normal embryos at the same stages of development.

The migration of the cells from the nodose placode to form the nodose ganglion was not observed in explants exposed to *int-2* antisense, whereas antisense treatment *in vivo* resulted in a delay in the development of the nodose ganglion with a concomitant reduction in its size. This is a prototypical example showing that the observation of developmental phenomena *in vivo* constitute an important extension of those *in vitro* because of the limitations imposed by explantation experiments, which at the least include time and factor dilution. *Int-2* is most likely serving as a diffusible factor and must traverse the distance between the rhombencephalon and otic/nodose placodes. Thus, in explants with three cut surfaces like the ones in these experiments, it is possible that many factors are

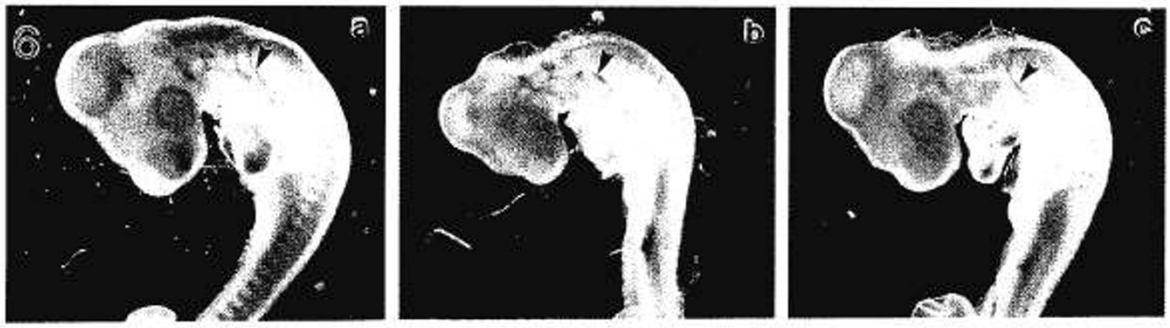

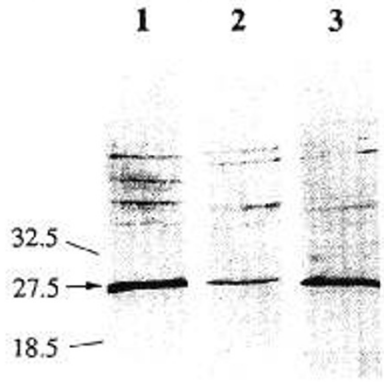

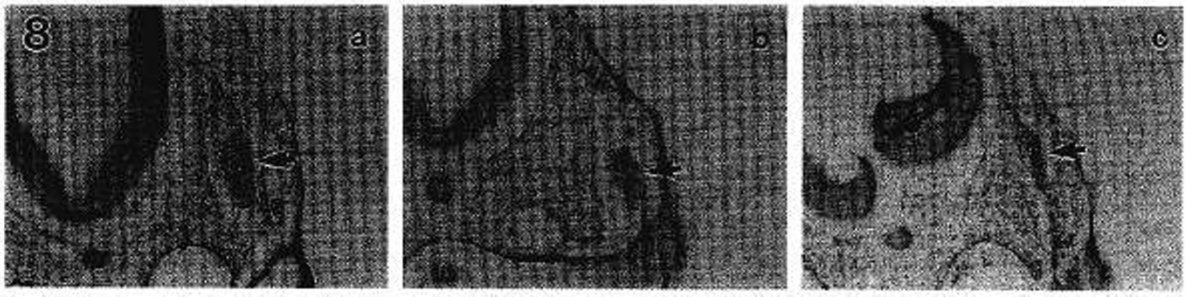

Figure 6. Immunostaining of neurofilament in whole-mount embryos. *a*, Embryo (stage 18) without exposure to oligonucleotide. The nerve trunks of the cranial sensory ganglia are brown. The nodose ganglion is located just posterior to the petrosal ganglion and is connected to the neural tube by the vagus nerve. *b* Embryo exposed to *int-2* antisense oligonucleotide. The vagus nerve does not connect the nodose ganglion to the neural tube. A connection can be seen between the nodose and petrosal ganglion; however, the petrosal ganglion also lacks a central connection. *c*, Embryo exposed to *int-2* sense oligonucleotide. The vagus nerve has formed normally. Nodose ganglia are indicated by *arrowheads*.

Figure 7. Western blot showing human *int-2* antibody identifies a protein of 27.5 kD in chick. *Lane 1*, stage 18 normal embryos. *Lane 2*, stage 18 embryos exposed to *int-2* antisense oligonucleotide. *Lane 3*, stage 18 embryos exposed to *int-2* sense oligonucleotide. Equal amounts of protein were loaded in each lane.

Figure 8. Peroxidase/anti-peroxidase immunostaining using antibody to human *int-2* in the pharyngeal region of chick embryos. Immunoreactivity can be seen in the nodose ganglia of stage 18 normal embryos (*a*). The *int-2* immunoreactivity of the nodose ganglia is reduced in the embryos exposed to *int-2* antisense oligonucleotide (*b*). Embryos exposed to *int-2* sense oligonucleotide were used as control (*c*), and these show *int-2* immunoactivity in the nodose ganglia comparable to that in normal embryos. The nodose ganglia are indicated by the *arrows*. Bar = 120 μm.

diluted. Since comparable *in vivo* data were not available in previous experiments showing abnormal development of the otocyst in chick explants, it is unclear whether this should be taken as a definitive result (our unpublished observations) (9).

This situation is emphasized further by the discrepancy between chicks exposed to *int-2* antisense oligonucleotides and antibody which show abnormal formation of the otocyst in explants, and in intact mice embryos lacking *int-2* expression which show dramatic differences in development of the ear, even though closure of the otocyst is normal (12). The discrepancy could be due to the limitations imposed by *in vitro* culture, in the case of the chick, as exemplified by the difference in our results in explants *versus* intact animals. An alternative explanation for the difference could be the result of a slight timing difference in the window of competency for induction of otocyst formation by *int-2*, or induction of otocyst closure by a different, but related, factor in the mouse *versus* chick. Since *int-2* is a member of the FGF family, it would not be surprising if other members of the family perform overlapping inductions in different species of animals.

Represa *et al.* (9) showed that FGF-2 can mimic the inductive signal in the absence of the rhombencephalon to induce the formation of the otocyst. Proteins in the FGF family share a common structure, and their amino acids are highly conserved. Many heterologous FGFs, including *int-2*, show mesoderm-inducing activity (20, 21). All members of the family, apart from FGF-1 and FGF-2, contain a signal peptide at their amino terminus, which directs passage through the secretory pathway

(22). The biologic activities of FGF-1 and FGF-2 are mediated through high affinity cell surface receptors that have an associated tyrosine kinase activity (23). Four members of the FGF receptor family have been cloned and found to be encoded by a family of related genes. Different members of the FGF family bind different FGF receptors with different affinities (23, 24). It is unclear if *int-2* acts by binding and activating FGF receptors.

Mansour *et al.* (12) proposed that the the experiments by Represa *et al.* (9), who used antisense sequence and antibodies for human and mouse *int-2*, were not valid because of nonexistence or sequence divergence of the *int-2* gene in chick. By cloning this portion of the chick *int-2* gene, we have shown that the sequence of the chick gene in the region of the antisense oligonucleotides used in our experiments and those of Represa *et al.* (9) should be effective. We do not know how much the gene has diverged beyond the boundaries of our clone, but even large differences should not be significant in the context of these antisense experiments.

While both otic and nodose placodes are undergoing important changes at about the same time, the morphogenetic events are quite distinct. The otic placode forms an otocyst while cells of the nodose placode delaminate to form the nodose ganglion. Although it is possible that two distinct morphogenetic processes are initiated by the same inducing protein, it is not likely. Both otocyst closure and subsequent development of the otocyst, and nodose ganglia formation, require proliferation of placodal cells, and it is more likely that *int-2* protein is involved in this. Even though initial formation of the otocyst is normal, inner ear and cochlear ganglion development is severely affected in the *int-2* mutant mouse. Thus the reemerging common themes of the present experiments with those of Represa *et al.* (9) and Mansour *et al.* (12) are timing and proliferation. In this regard, Represa *et al.* (9) noted the absence of mitotic activity in the presence of *int-2* antisense oligonucleotide, and *int-2* protein has been shown to promote DNA synthesis in quiescent cultures of mammary epithelial cells (19). The *int-2* protein is most likely a signal produced by cells in the rhombencephalon that is released and diffuses to the otic and nodose placodes (6, 18). The delayed development of the nodose ganglia in an environment with reduced *int-2* protein indicates that *int-2* may function to potentiate or stimulate the generation of cells from the nodose placode. This is consistent with the *int-2* mutant mouse where the facioacoustic ganglion primordium was much smaller than control ganglion.

At a slightly later stage of development, expression of *int-2* disappears from the rhombencephalon and *int-2* transcripts are localized in a thickened region of the otic vesicle that is destined to form the sensory tissue of the vestibular organ (8). Our data suggest that the protein is also expressed by cells generated from the nodose placode. Western analysis and immunohistochemical data show a reduction of *int-2* expression in the nodose ganglia 48 h after exposure of the rhombencephalon to *int-2* antisense oligonucleotide, suggesting that the initial expression of *int-2* in the rhombencephalon is required for *int-2* expression by the nodose placode derivatives. Wilkinson *et al.* (8) suggest that this later expression of *int-2* may be a factor involved in sensory cell differentiation and/or innervation. The absence of visible nerve trunks connecting the nodose ganglia to the medulla 3 d after treatment supports the idea that the expression of *int-2* by the nodose ganglion cells is important for normal development of the central processes of the nodose ganglion cells or recognition of the ganglion by the motor axons of the vagus nerve. It is possible that the processes emanating from, and directed to the nodose ganglion are defasciculated, and therefore were not detected in our sections, but this still indicates a role for *int-2* in normal development of the nerve trunks of the nodose ganglia. The delayed appearance and decrease in size of the nodose ganglia initially, followed several days later by absence or defasciculation of the vagus nerve connecting the ganglion with the brainstem supports the idea of a two-step model for *int-2* induction, proposed by Wilkinson *et al.* (8), for the development of the inner ear.

Our interest in factors common to the generation of the nodose ganglia and inner ear arises from a surgical model of the long QT syndrome which occurs with or without deafness (14, 25). A surgical model of the long QT is created by ablation of the nodose placodes before formation of the nodose ganglia (14, 15). If the lesion is extended slightly to encroach on the otic placodes, these embryos also frequently have congenital deafness, as measured by electrocochleography (26). The prolonged QT interval is associated with decreased vagal sensory innervation of the heart (15, 26). Thus, proteins affecting the development of both of these placodes are genetic candidates to underlie this condition.

An imbalance in the sympathetic innervation to the heart is thought to cause long QT syndrome (27). The innervation of the chick heart is from at least three sets of nerves (28). Postganglionic cardiac sympathetic nerves are found in the first thoracic sympathetic ganglia of the paravertebral sympathetic trunks. The parasympathetic postganglionic cardiac nerves are located on the surface of the heart. Sensory innervation to the heart arises predominately from the nodose ganglia. Kessler *et al.* showed that the density of autonomic and sensory innervation in an end organ is modulated by reciprocal interactions that involve competition for growth factors among the nerve terminals in that end organ. They removed sensory, parasympathetic, or sympathetic innervation from the iris and showed hypertrophic growth of all the remaining innervation. The explanation for this result was that removal of any one set of nerves reduced the level of competition in the end organ for growth factors, and resulted in added growth of the remaining nerves (29, 30). A similar phenomenon has been shown to occur in the developing heart (31). This provides the basis for one hypothesis for the embryogenesis of the long QT syndrome, which is that an imbalance of sympathetic innervation to the heart arises when the nodose ganglia do not form normally.

We attempted to maintain some of our antisense-treated embryos alive to a stage when the EKG and electrocochleograms could be measured; however, no embryos in the *int-2* antisense group survived to 12 d after the surgery, even though some from the control groups did survive to d 12. The reason for this degree of mortality is not known, but parallels that seen *int-2* deficient mice. The delayed development of the nodose ganglia and otocysts in embryos exposed to *int-2* antisense oligonucleotides may provide a molecular basis to explain one etiology of the long QT syndrome.

Acknowledgments. The authors thank Harriett Stadt, Donna Kumiski, Kathleen Wallis, and Noboru Mishima for technical assistance, and Karen Waldo for the graphic arts.

REFERENCES

1. Peters G, Brookes S, Smith R, Dickson C 1983 Tumorigenesis by mouse mammary tumor virus: Evidence for a common region for provirus integration in mammary tumors. Cell 33:369–377
2. Dickson C, Smith R, Brookes S, Peters G 1984 Tumorigenesis by mouse mammary tumor virus: proviral activation of a cellular gene in the common integration region *int-2*. Cell 37:529–536
3. Dickson C, Peters G 1987 Potential oncogene product related to growth factors. Nature 326:833
4. Goldfarb M 1990 The fibroblast growth factor family. Cell Growth Differ 1:439–445
5. Tannahill D, Isaacs HV, Close MJ, Peters G, Slack JMW 1992 Developmental expression of the Xenopus *int-2* (FGF-3) gene: activation by mesodermal and neural induction. Development 115:695–702
6. Wilkinson DG, Peters G, Dickson C, McMahon AP 1988 Expression of the FGF-related proto-oncogene *int-2* during gastrulation and neurulation in the mouse. EMBO J 7:691–695
7. Niswander L, Martin GR 1992 FGF-4 expression during gastrulation, myogenesis, limb and tooth development in the mouse. Development 114:755–768
8. Wilkinson DG, Bhatt S, McMahon AP 1989 Expression pattern of the FGF-related proto-oncogene *int-2* suggests multiple roles in fetal development. Development 105:131–136
9. Represa J, León Y, Miner C, Giraldez F 1991 The *int-2* proto-oncogene is responsible for induction of the inner ear. Nature 353:561–563
10. Verwoerd C, Van Oostrom C 1979 Cephalic neural crest and placodes. Adv Anat Embryol Cell Biol 58:1–75
11. Webb JF, Noden DM 1993 Ectodermal placodes: contributions to the development of the vertebrate head. Am Zool 33:434–447
12. Mansour SL, Goddard JM, Capecchi MR 1993 Mice homozygous for a targeted disruption of the proto-oncogene *int-2* have developmental defects in the tail and inner ear. Development 117:13–28
13. d'Amico-Martel A, Noden DM 1983 Contribution of placodal and neural crest cells to avian cranial peripheral ganglia. Am J Anat 166:445–468
14. Christiansen JL, Stadt HA, Mulroy MJ, Kirby ML 1989 Electrocardiographic QT prolongation after ablation of the nodose placode in the chick embryo: A developmental model of the idiopathic long QT syndrome Pediatr Res 26:11–15
15. Mulroy MJ, Hotelling HB, and Harrison TA 1990 Long QT and long QT with deafness syndrome: Beginning a neural analysis in an embryonic chick model. NY Acad Sci 588:430–432
16. Jervell A, Lange-Nielsen F 1957 Congenital deaf-mutism, functional heart disease with prolongation of the Q-T interval and sudden death. Am Heart J 54:59–68
17. Romano C, Gemme G, Pongiglione R 1963 Aritmie cardiache rare dell'eta pediatrica. Vlin Paediatr 45:656–683
18. Harrison TA, Stadt HA, Kirby ML 1994 Developmental characteristics of the chick nodose ganglion. Int J Dev Neurosci 16:67–73
19. Dixon M, Deed R, Acland P, Moore R, Whyte A, Peters G, Dickson C 1989 Detection and characterization of the fibroblast growth factor-related oncoprotein *int-2*. Mol Cell Biol 9:4896–4902
20. Slack JMW, Darlington BG, Heath JK, Godsave SK 1987 Mesoderm induction in early Xenopus embryos by heparin-binding growth factors. Nature 326:197–200
21. Peterno GD, Gillespie LL, Dixon MS, Slack JMW, Heath JK 1989 Mesoderm-inducing properties of *int-2* and kFGF: two oncogene-encoded growth factors related to FGF. Development 106:79–83
22. Dickson C, Acland P, Smith R, Dixon M, Deed R, Macallan D, Walther W, Fuller-Pace F, Kiefer P, Peters G 1990 Characterization of *int-2*: a member of the fibroblast growth factor family. J Cell Sci Suppl 13:87–96
23. Coughlin SR, Barr PJ, Cousens LS, Fretto LJ, Williams LT 1988 Acidic and basic fibroblast growth factors stimulated tyrosine kinase activity *in vivo*. J Biol Chem 263:988–993
24. Vainikka S, Partanen J, Bellosta P, Coulier F, Basilico C, Jaye M, Alitalo K 1992 Fibroblast growth factor receptor-4 shows novel features in genomic structure, ligand binding and signal transduction. EMBO J 11:4273–4280
25. Mulroy MJ, Harrison TA 1994 Developmental study of the long QT with deafness syndrome in the chick embryo: cochlear pathology Int J Pediatr Otorhinolaryngol 29:179–194
26. Mulroy MJ and Harrison TH 1991 Decreased vagal sensory innervation of the heart is associated with prolonged QT intervals in the electrocardiogram. Neuroscience 17:284(abstr)
27. Schwartz PJ 1985 Idiopathic long QT syndrome: progress and questions. Am Heart J 109:399–411
28. Kirby ML and Stewart DE 1986 Development of the ANS innervation to the avian heart. In: Clifton GP (ed) Developmental Neurobiology of the Autonomic Nervous System. Totowa, NJ, Humana Press, pp. 135–158
29. Kessler JA 1985 Parasympathetic, sympathetic, and sensory interactions in the iris: nerve growth factor regulates cholinergic ciliary ganglion innervation *in vivo*. J Neurosci 5:2719–2725
30. Kessler JA, Bell WO, Black IB 1983 Interactions between sympathetic and sensory innervation of the iris. J Neurosci 3:1301–1307
31. Kirby ML, Conrad DC, Stewart DE 1987 Increase in the cholinergic cardiac plexus in sympathetically aneural hearts. Cell Tissue Res 247:489–496